Supporting Information

Highly Functional Ellipsoidal Block Copolymer Nanoparticles: A Generalized Approach to Nanostructured Chemical Ordering in Phase Separated Colloidal Particles

*Bernhard V. K. J. Schmidt, Cynthia X. Wang, Stephan Kraemer, Luke A. Connal and Daniel Klinger**

Dr. Bernhard V.K.J. Schmidt, Cynthia X. Wang, Dr. Stephan Kraemer
Materials Research Laboratory, University of California, Santa Barbara, CA 93106, USA

Prof. Luke A. Connal
Research School of Chemistry, Australian National University, Canberra, Australian Capital Territory, Australia, 2601

Prof. Daniel Klinger
Institute of Pharmacy, Freie Universität Berlin, Königin-Luise-Str. 2-4, 14195 Berlin, Germany, e-mail: daniel.klinger@fu-berlin.de

Content

1. Synthesis of P2VP-selective surfactant for striped ellipsoidal PS-b-P2VP nanoparticles

*Synthesis of 16-Hydroxy-*N,N,N*-triethylhexadecan-1-ammonium bromide (CTEAB-OH)[1]*

16-Bromo-1-hexadecanol (1.00g, 3.11 mmol, 1.0 eq.) was dissolved in ethyl acetate (12 mL) and triethylamine (6.8 mL, 49.56 mmol, 15.7 eq.) was added. The reaction mixture was stirred in a sealed tube at 60 °C under argon for 16 d. Subsequently, the mixture was filtered, the obtained solid was dried in the vacuum oven at 40 °C and recrystallized from a 2:1 mixture of diethylether/ethanol (15 mL) to obtain the product as a white solid (0.73 g, 1.72 mmol, 55%). ^{1}H NMR (500 MHz, CD_3OD, *δ*): 3.53 (t, *J*=6.7 Hz, 2H; C**H**$_2$-OH), 3.37-3.27 (m, 7H; C**H**$_2$-CH$_3$, O**H**), 3.23-3.12 (m, 2H; C**H**$_2$-N), 1.74-1.62 (m, 2H; C**H**$_2$-CH$_2$-N), 1.58-1.47 (m, 2H; C**H**$_2$-CH$_2$-O), 1.46-1.23 (m, 31H; 11xC**H**$_2$, 3xC**H**$_3$); ^{13}C NMR (126 MHz, CD_3OD, δ): 61.6 (**C**H$_2$-OH), 56.7 (CH$_2$-**C**H$_2$-N), 52.5 (**C**H$_2$-CH$_3$), 52.4 (**C**H$_2$-CH$_3$), 52.4 (**C**H$_2$-CH$_3$), 32.3 (**C**H$_2$-CH$_2$-OH), 29.3 (**C**H$_2$), 29.3 (**C**H$_2$), 29.2 (**C**H$_2$), 29.2 (**C**H$_2$), 29.2 (**C**H$_2$), 28.8 (**C**H$_2$), 26.1 (**C**H$_2$-CH$_2$-N), 25.5 (CH$_2$), 21.3 (**C**H2), 6.3 (**C**H$_3$). MS (ESI) *m*/*z*: [M]$^+$ calcd for $C_{22}H_{48}NO$, 342.3736; found, 342.3726.

2. Synthesis of functional copolymers

2.1. Synthesis of benzyl dodecyl trithiocarbonate (BDT)

BDT was synthesized via a modified literature procedure.[2, 3] Dodecanethiol (4.7 mL, 19.8 mmol, 1.1 eq.) was added to a suspension of potassium phosphate (4.2 g, 19.7 mmol, 1.1 eq.) in acetone (100 mL). After 10 min, carbon disulfide (3.2 mL, 53.9 mmol, 3.0 eq.) was added via syringe. The mixture was stirred for another 20 min, benzyl bromide (2.1 mL, 18.0 mmol, 1.0 eq.) was added and the mixture was stirred over night at ambient temperature. HCl (100 mL) was added and the aqueous phase extracted two times with DCM (250 mL). The organic phase was washed with deionized water (200 mL), brine (200 mL) and dried over Na_2SO_4. The organic phase was evaporated, dissolved in a 1:1 mixture of acetone and hexane

(40 mL), NEt_3 (2.3 mL, 18.0 mmol, 1.0 eq.) and a pinch of NaI was added. The mixture was stirred over night, evaporated and the residue subjected to column chromatography on silica gel with hexane as eluent. The corresponding fractions were merged and evaporated to yield the product as a yellow oil that crystallized in the fridge to afford yellow needles (2.83 g, 7.7 mmol, 43%). ^{1}H NMR (500 MHz, $CDCl_3$, *δ*): 7.42-7.19 (m, 5H; Ar **H**), 4.62 (s, 2H; C**H**$_2$-Ph), 3.37 (t, *J* = 7.4 Hz, 2H; CH_2-C**H**$_2$-S), 1.79-1.62 (m, 2H; C**H**$_2$-CH_3), 1.47-1.19 (m, 18H; C**H**$_2$), 0.89 (t, *J* = 6.6 Hz, 3H; C**H**$_3$); ^{13}C NMR (126 MHz, $CDCl_3$, δ): 223.7 (**C**=S), 135.1 (**C**-CH_2-S), 129.2 (Ar **C**H), 128.7 (Ar **C**H), 127.7 (Ar **C**H), 41.4 (**C**H_2-Ph), 37.1 (CH_2-**C**H_2-S), 31.9 (**C**H_2), 29.6 (**C**H_2), 29.6 (**C**H_2), 29.5 (**C**H_2), 29.4 (**C**H_2), 29.3 (**C**H_2), 29.1 (**C**H_2), 28.9 (**C**H_2), 28.0 (**C**H_2), 22.7 (**C**H_2-CH_3), 14.1 (**C**H_3). MS (EI) *m/z*: $[M]^+$ calcd for $C_{20}H_{32}S_3$, 368.1666; found, 368.1656.

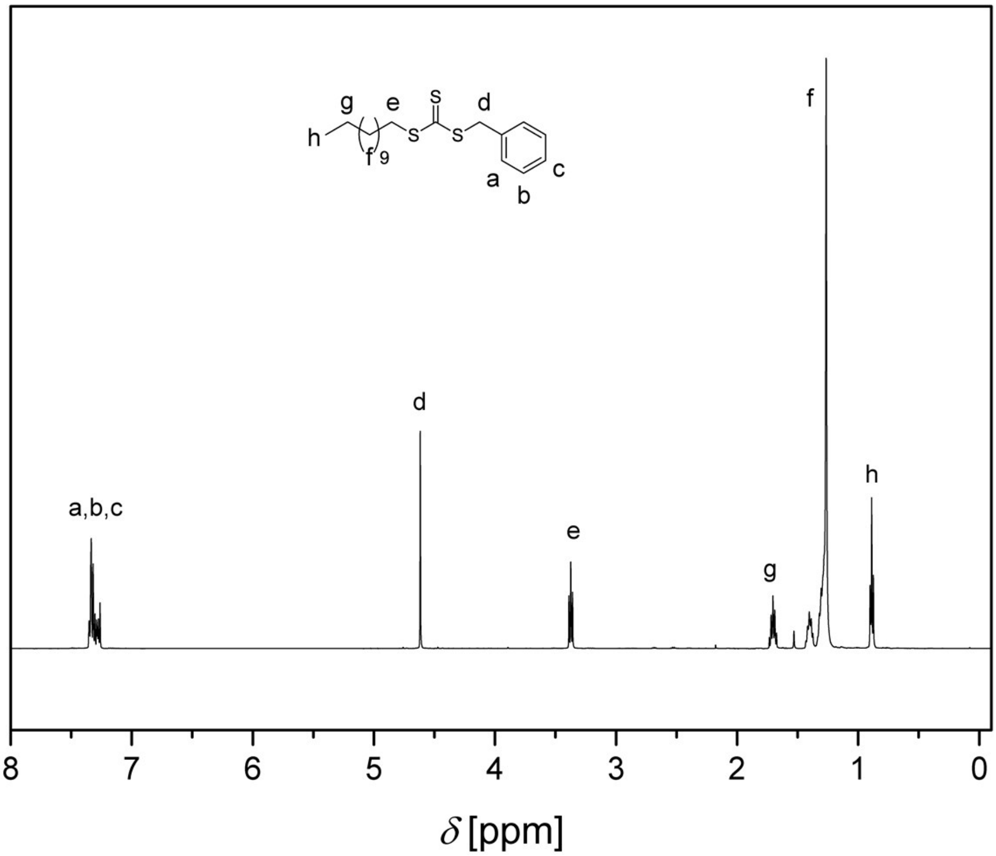

Figure S1. ^{1}H-NMR spectrum of BDT in $CDCl_3$ at 500 MHz.

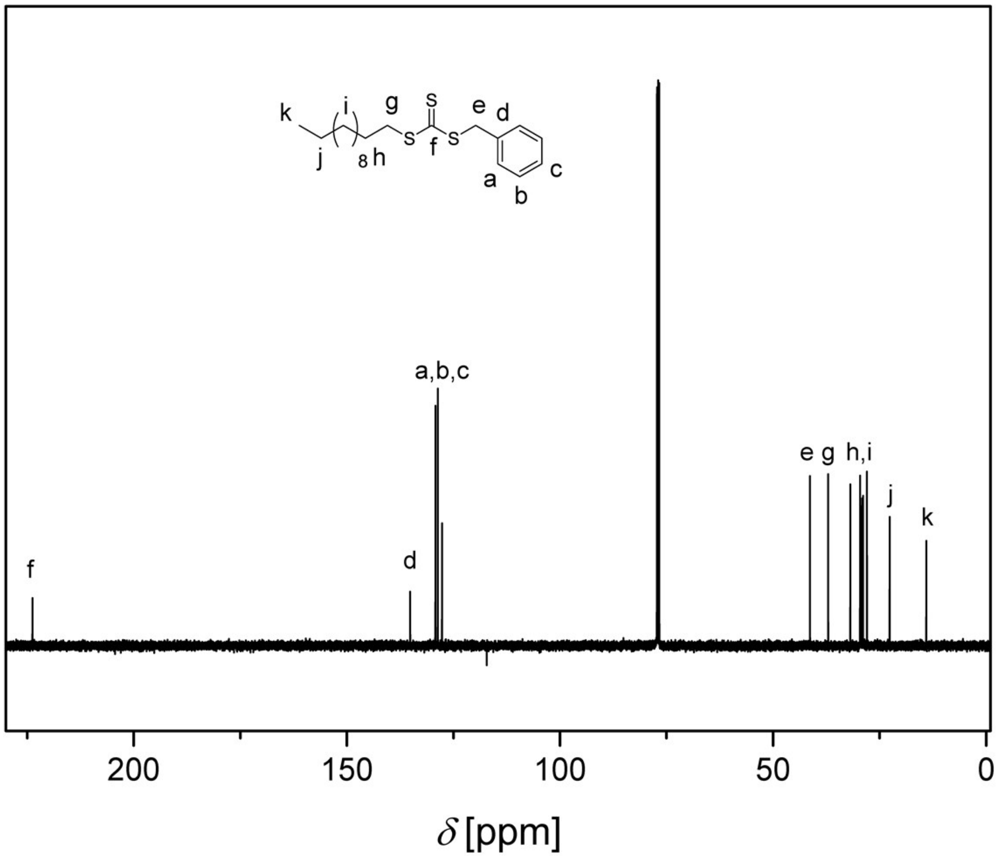

Figure S2. ^{13}C-NMR spectrum of BDT in $CDCl_3$ at 126 MHz.

2.2. Synthesis of 4-vinyl benzophenone (VBz)[4]

In a 250 mL Schlenk flask potassium trimethylsilanolate (9.85 g, 76.64 mmol, 3.5 eq.), palladium tris(dibenzylideneacetone) (500 mg, 0.55 mmol, 0.025 eq.) and triphenylphosphine oxide (305 mg, 1.09 mmol, 0.05 eq.) were dissolved in dry THF (44 mL) under argon. 4-Bromobenzophenone (5.71 g, 21.90 mmol, 1.0 eq.) and 1,3-divinyltetramethyldisiloxane (5.6 mL, 24.16 mmol, 1.1 eq.) were added under stirring. The mixture was stirred at 70 °C for 5 h. Subsequently, diethylether (50 mL) was added and the mixture was stirred for 5 min. Finally, the mixture was filtered over a short silica gel pad, the silica gel pad was flushed with diethylether (200 mL) and the solvent was evaporated in vacuo. The crude product was subjected to column chromatography on silica gel with a gradual change of the eluent hexane/DCM from 88% to 0% to afford VBz as slightly green solid after cooling in the freezer (3.94 g, 18.93 mmol, 87%). ^{1}H NMR (500 MHz, $CDCl_3$, δ): 7.83-7.74 (m, 4H; Ar-**H**), 7.62-7.55 (m, 1H; Ar-**H**), 7.53-7.45 (m, 4H; Ar-**H**), 6.79 (dd, *J*=17.6 Hz, *J*=10.9 Hz, 1H; C**H**-CH_2), 5.89 (d, *J*=17.6 Hz, 1H; C$\mathbf{H}_{cis}$), 5.41 (d, *J* = 11.0 Hz, 1H; C$\mathbf{H}_{trans}$); ^{13}C NMR (126 MHz, $CDCl_3$, δ): 196.1 (**C**=O), 141.5 (**C**-CH-CH_2), 137.8 (**C**-C=O), 136.7 (**C**-C=O), 136.0 (H**C**=CH_2), 132.3 (Ar-**C**H), 130.5 (Ar-**C**H), 129.9 (Ar-**C**H), 128.3 (Ar-**C**H), 126.0 (Ar-**C**H), 116.6 (**C**H_2=CH). MS (ESI) *m/z*: $[M+Na]^+$ calcd for $C_{15}H_{12}ONa$, 231.0786; found, 231.0776.

2.3. *Exemplary RAFT copolymerization of 2VP and VBz (P2VP-*co*-VBz-1)*

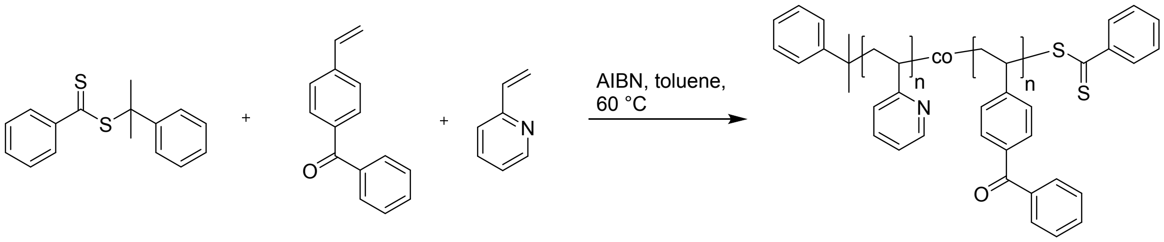

Scheme S1. Photocrosslinker synthesis and synthesis of functionalized polymers: synthesis of P2VP-*co*-VBz via RAFT copolymerization of 2VP and VBz.

2VP (750 mg, 7.1 mmol, 1208.9 eq.), VBz (149 mg, 0.72 mmol, 122.6 eq.), AIBN (0.4 mg, 0.0024 mmol, 0.4 eq.), CDB (1.6 mg, 0.0059 mmol, 1.0 eq.) and toluene (750 mg) were mixed in a 5 mL Schlenk flask. The mixture was degassed via 4 freeze-pump-thaw cycles in the dark. Subsequently, argon was added, the flask was sealed and the mixture was heated to 60 °C under stirring for 24 h in the dark. The reaction was quenched with liquid nitrogen and the mixture precipitated in an excess of cold hexane. The precipitate was dissolved in a minimum amount of DCM and precipitated in an excess of cold diethylether. Finally the product was dried in the vacuum oven at 40 °C overnight to yield the product as pink solid (300 mg) and the product was kept in the dark for storage. A benzophenone incorporation of 15 mol% was calculated according to ^{1}H-NMR. SEC($CHCl_3$): M_n(SEC) = 32500 g mol^{-1}, $Đ$ = 1.42.

Table S1. Characterization of P2VP-based photocrosslinker polymers.

No.	M_n [g mol^{-1}] [a)]	$Đ$ [a)]	VBz content [mol-%] [b)]
P2VP-*co*-VBz-1	32500	1.42	15
P2VP-*co*-VBz-2	42900	1.44	26
P2VP-*co*-VBz-3	26600	1.39	37
P2VP-*co*-VBz-4	52500	1.41	50

a) measured via SEC in chloroform relative to PS standards, b) calculated from ^{1}H-NMR.

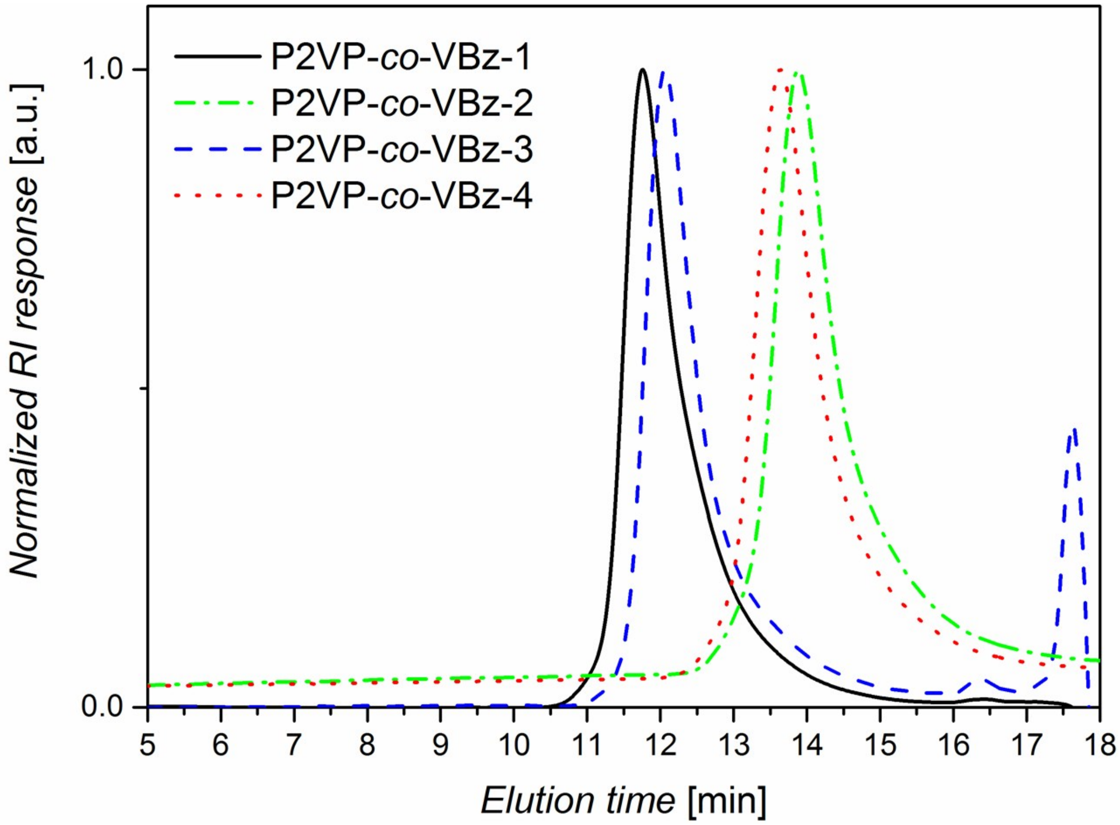

Figure S3. SEC elugrams of P2VP-*co*-VBz measured in chloroform.

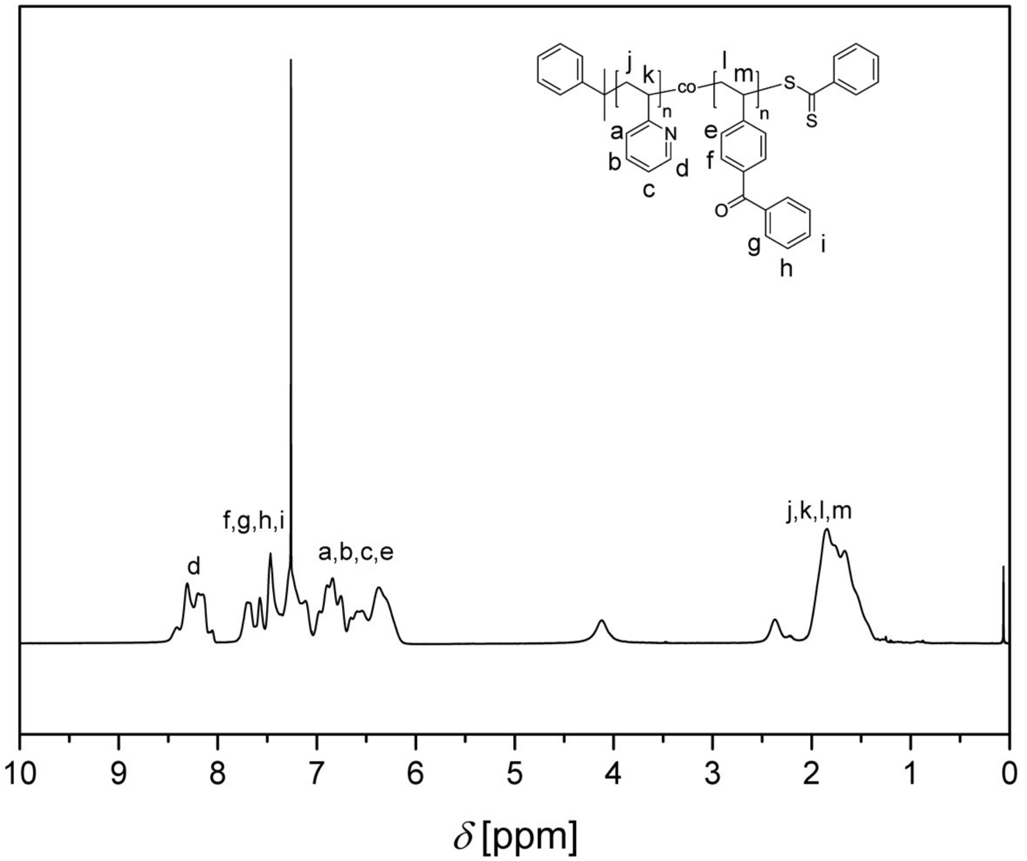

Figure S4. ^{1}H-NMR spectrum of P2VP-*co*-VBz-1 in $CDCl_3$ at 500 MHz.

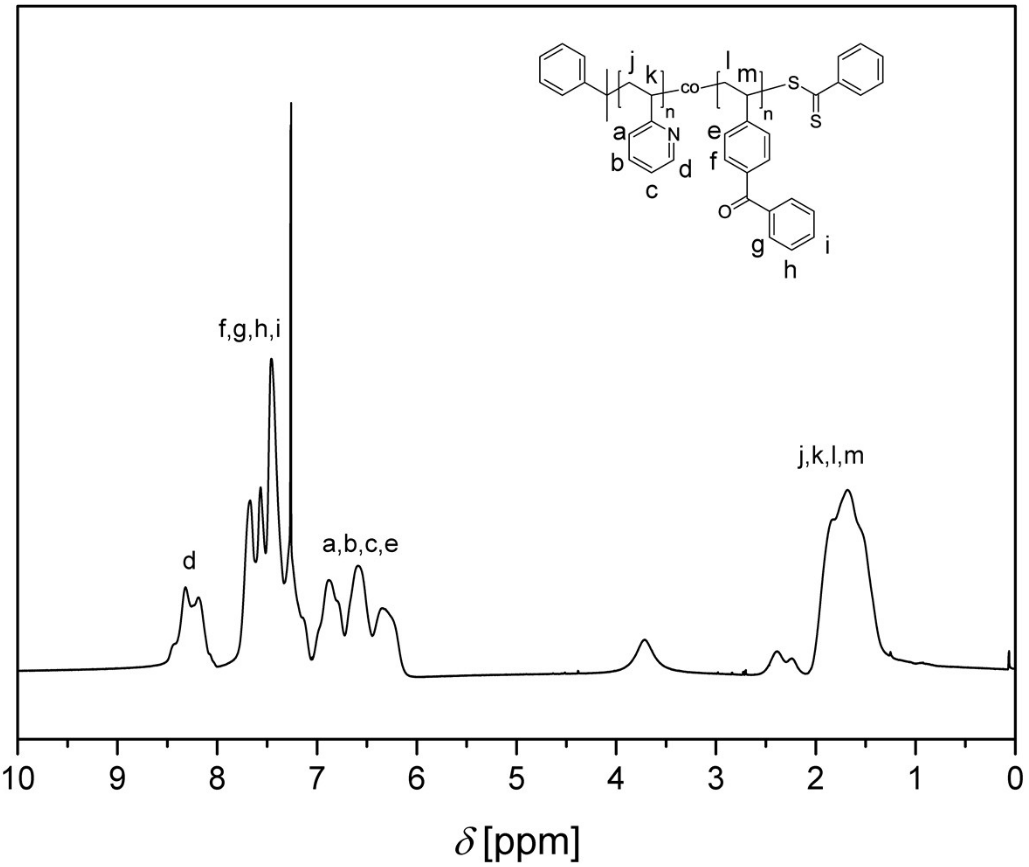

Figure S5. ^{1}H-NMR spectrum of P2VP-*co*-VBz-2 in $CDCl_3$ at 500 MHz.

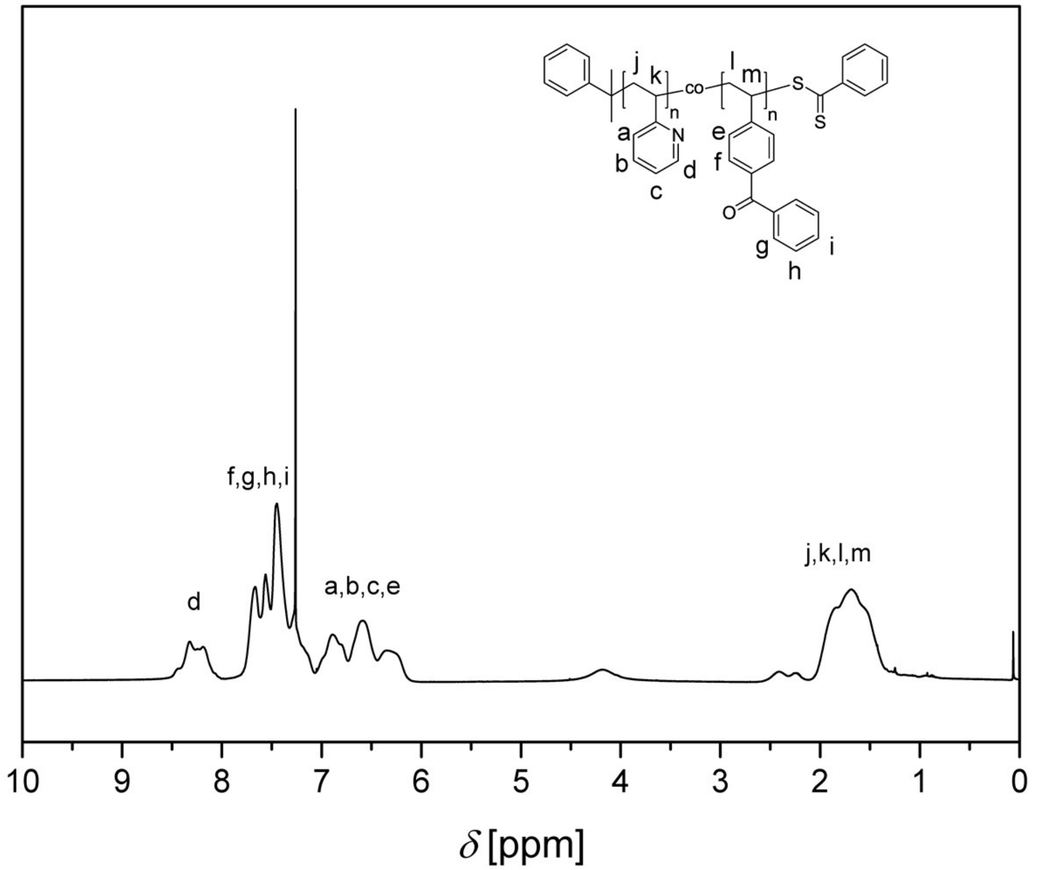

Figure S6. ^{1}H-NMR spectrum of P2VP-*co*-VBz-3 in $CDCl_3$ at 500 MHz.

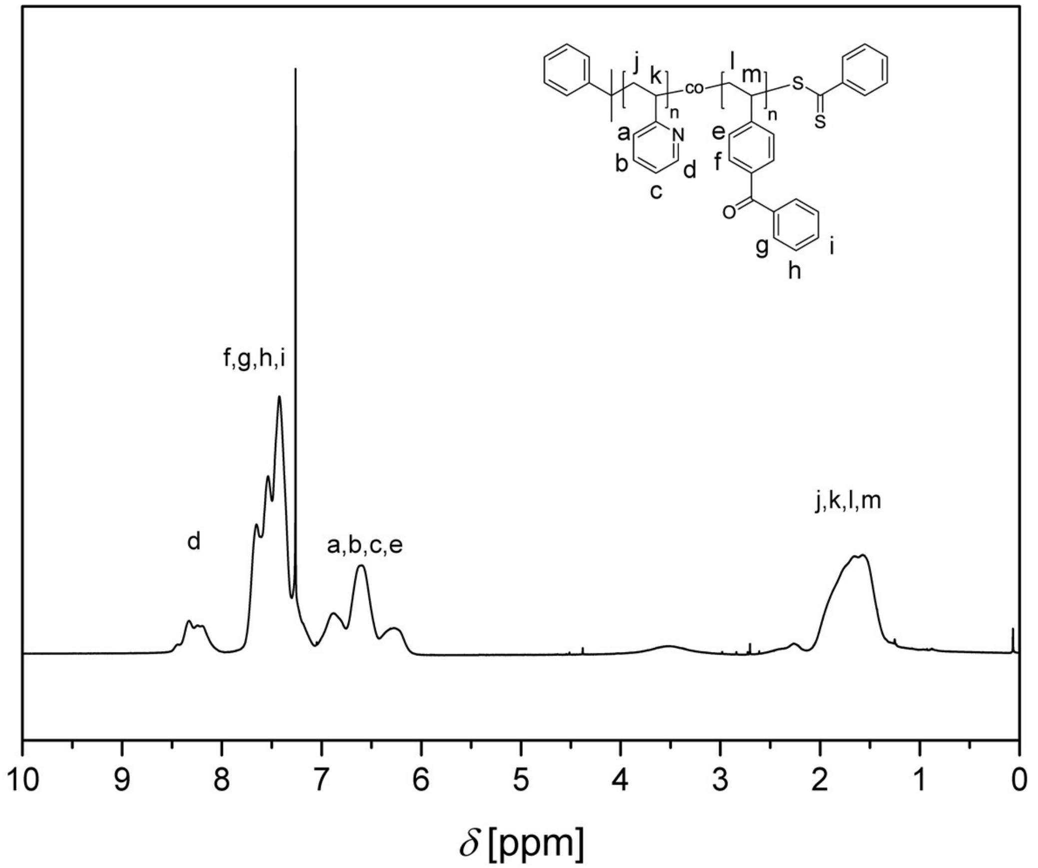

Figure S7. ^{1}H-NMR spectrum of P2VP-*co*-VBz-4 in $CDCl_3$ at 500 MHz.

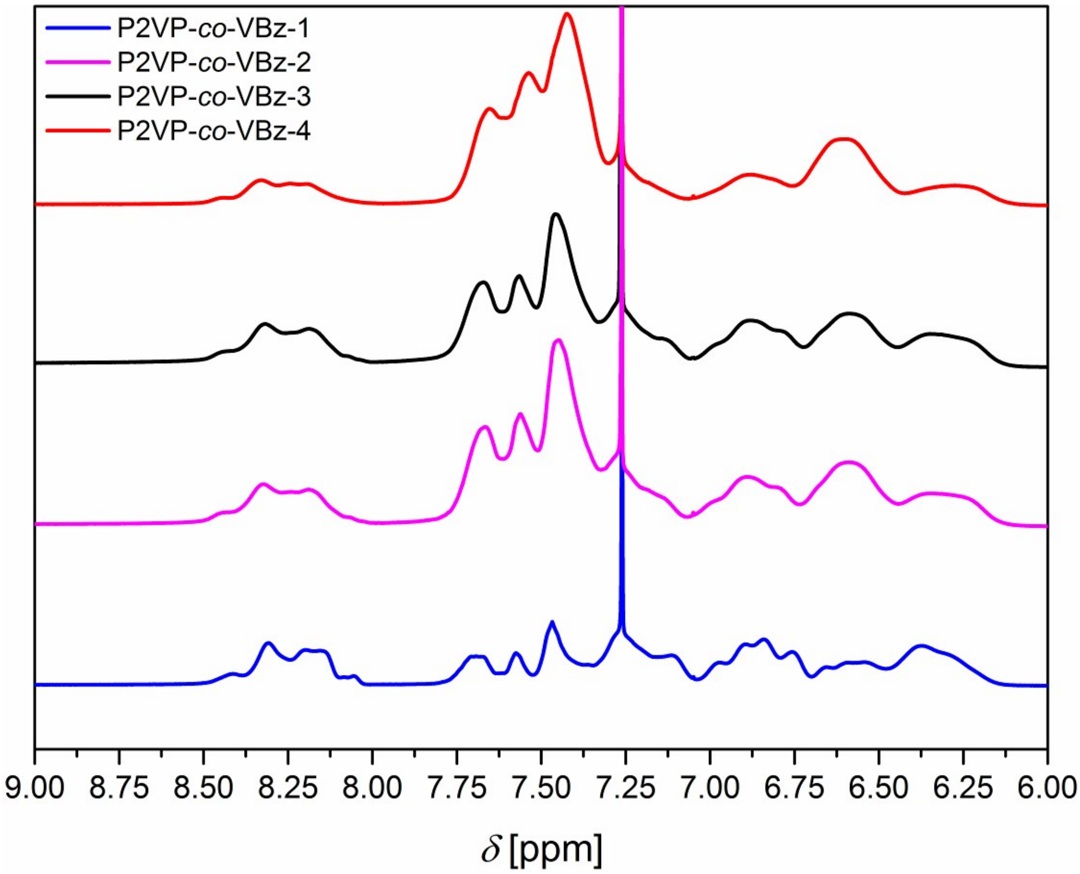

Figure S8. Collection of aromatic regions of ^{1}H-NMR spectra of P2VP-*co*-VBz in $CDCl_3$ at 500 MHz.

2.4. *Exemplary Friedel-Crafts acylation of PS (PS-*co*-VBz-1)*

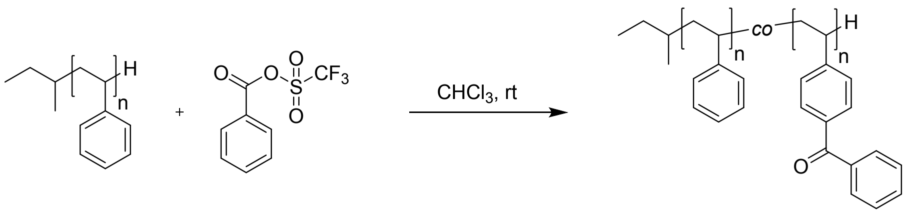

Scheme S2. Photocrosslinker synthesis and synthesis of functionalized polymers: a) synthesis of PS-*co*-VBz via Friedel-Crafts acylation.

According to the literature,[5] PS_{44k} (500 mg, 0.011 mmol, 1.0 eq.) was dissolved in dry chloroform (10 mL) in a dry 25 mL flask under argon. At ambient temperature benzoyl trifluoromethanesulfonate (246 mg, 0.968 mmol, 88.0 eq.) was added in the dark while stirring. The solution was stirred overnight and precipitated twice in an excess of cold methanol in the dark. Finally the product was dried in the vacuum oven at 40 °C overnight to give 380 mg of polymer and the product was kept in the dark for storage. A benzophenone incorporation of 15 mol% was calculated according to ^{1}H-NMR. SEC($CHCl_3$): M_n(SEC) = 53200 g mol^{-1}, $Đ = 1.15$.

Table S2. Characterization of PS-based photocrosslinker polymers.

No.	M_n [g mol^{-1}] [a)]	$Đ$ [a)]	VBz content [mol-%] [b)]
PS-*co*-VBz-1	53200	1.15	15
PS-*co*-VBz-2	63900	1.11	25
PS-*co*-VBz-3	69200	1.13	35
PS-*co*-VBz-4	71200	1.29	52

[a)] measured via SEC in chloroform relative to PS standards, [b)] calculated from ^{1}H-NMR.

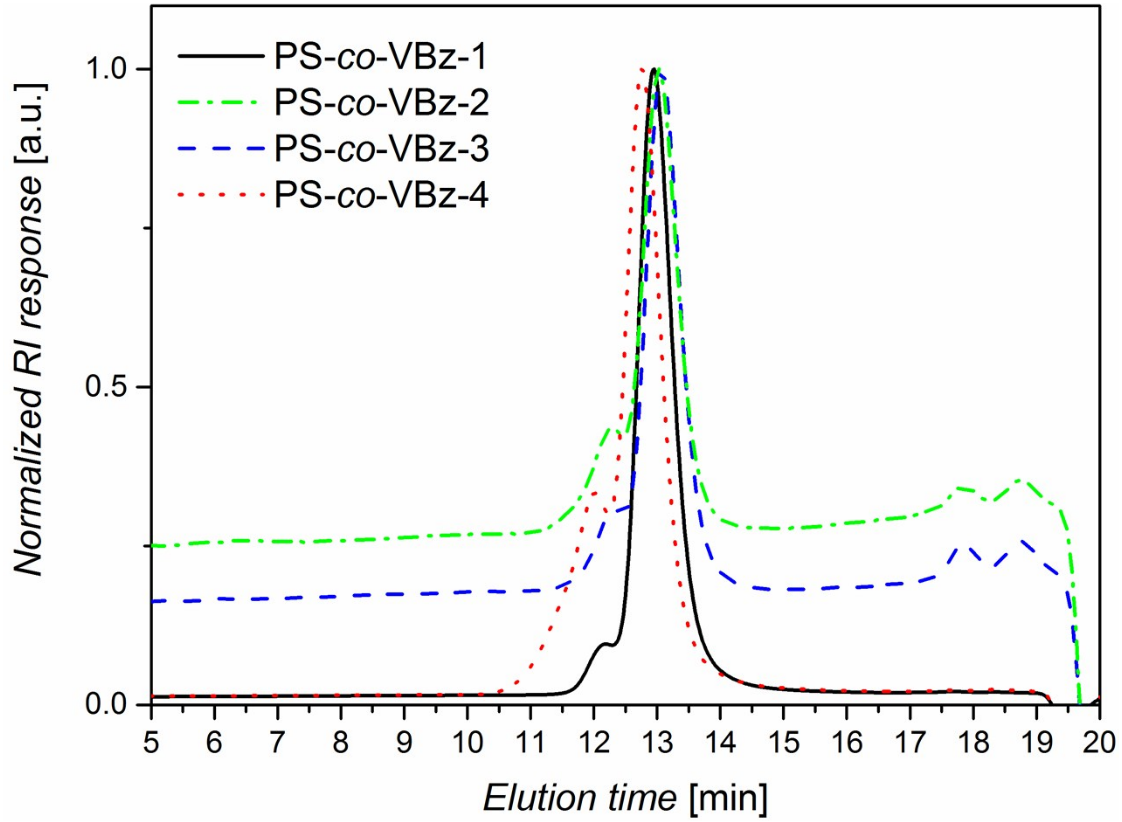

Figure S9. SEC elugrams of PS-*co*-VBz measured in chloroform.

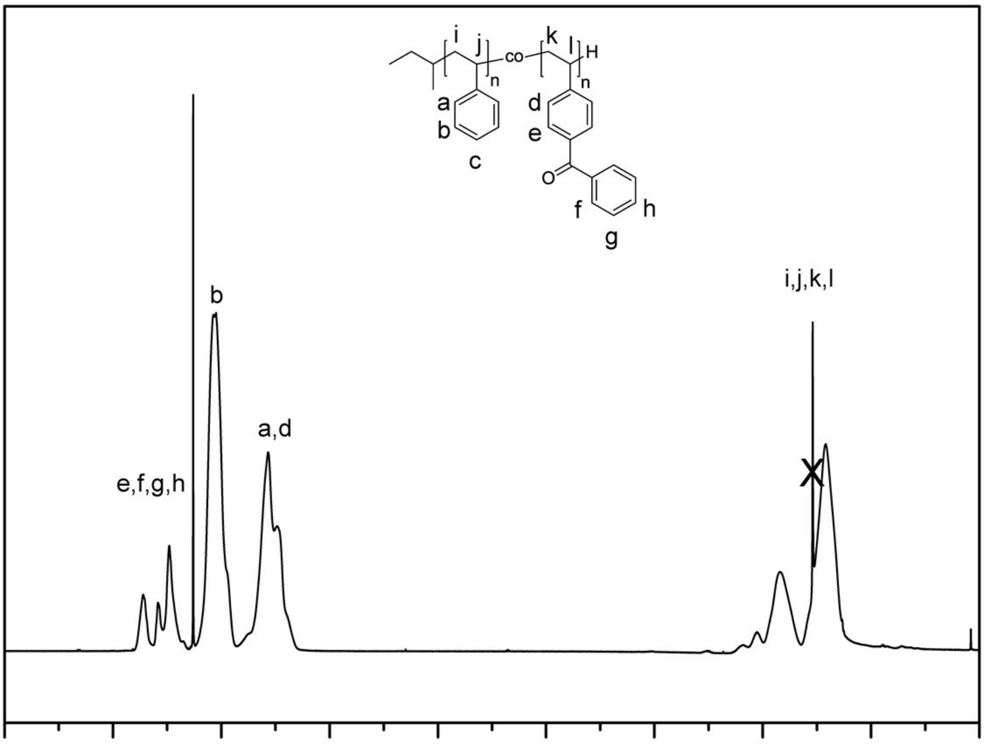

Figure S10. ^{1}H-NMR spectrum of PS-*co*-VBz-1 in $CDCl_3$ at 500 MHz.

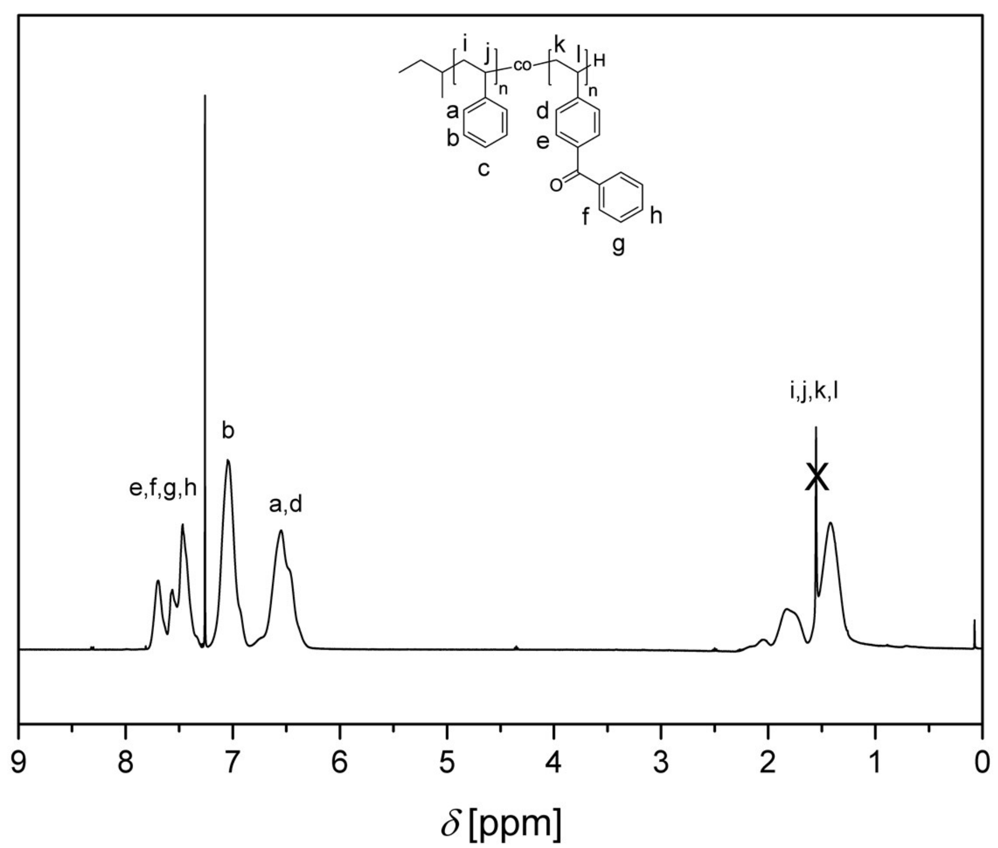

Figure S11. ^{1}H-NMR spectrum of PS-*co*-VBz-2 in $CDCl_3$ at 500 MHz.

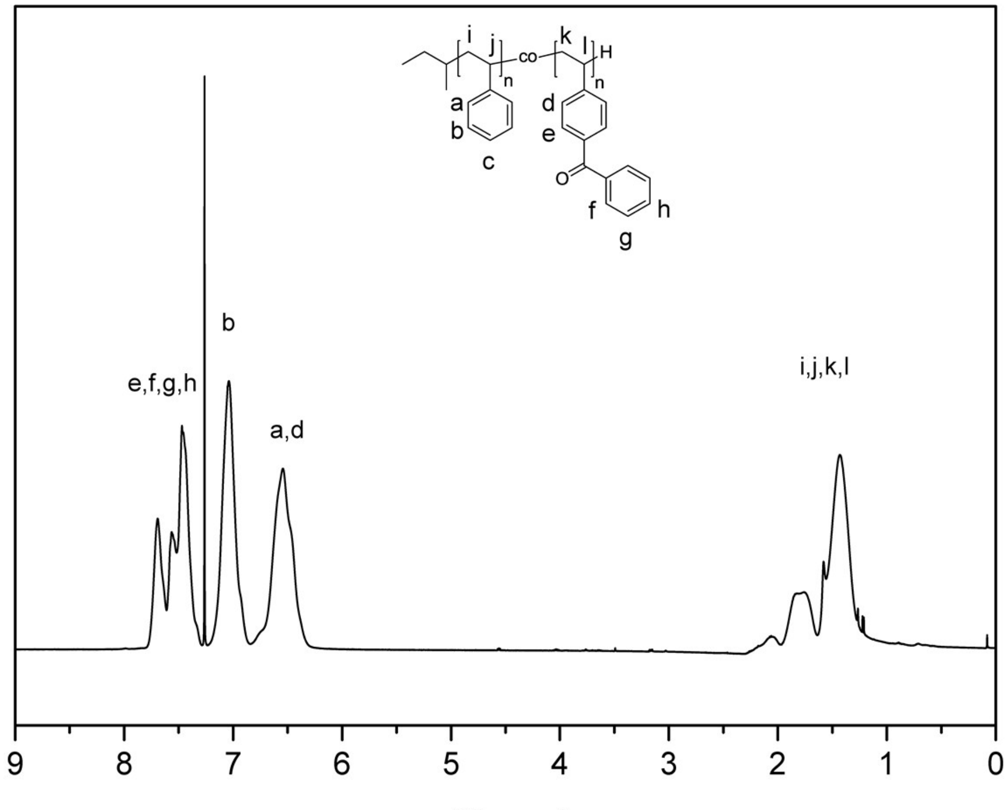

Figure S12. ^{1}H-NMR spectrum of PS-*co*-VBz-3 in $CDCl_3$ at 500 MHz.

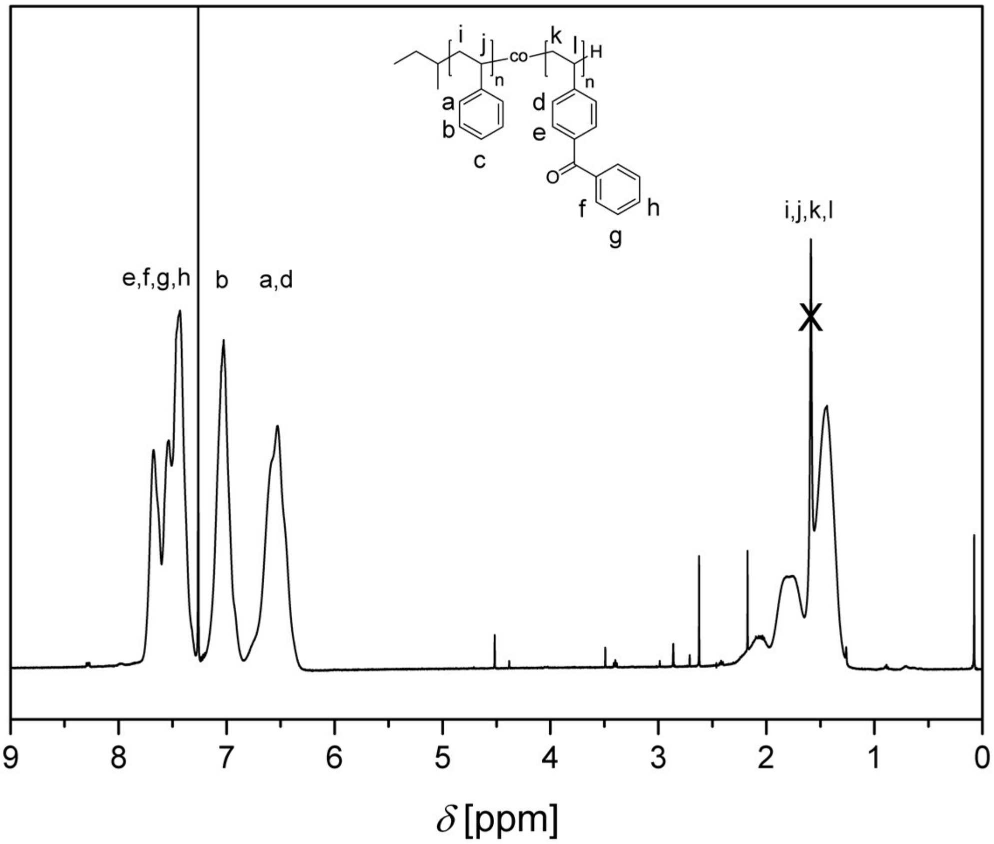

Figure S13. ^{1}H-NMR spectrum of PS-*co*-VBz-4 in CDCl$_3$ at 500 MHz.

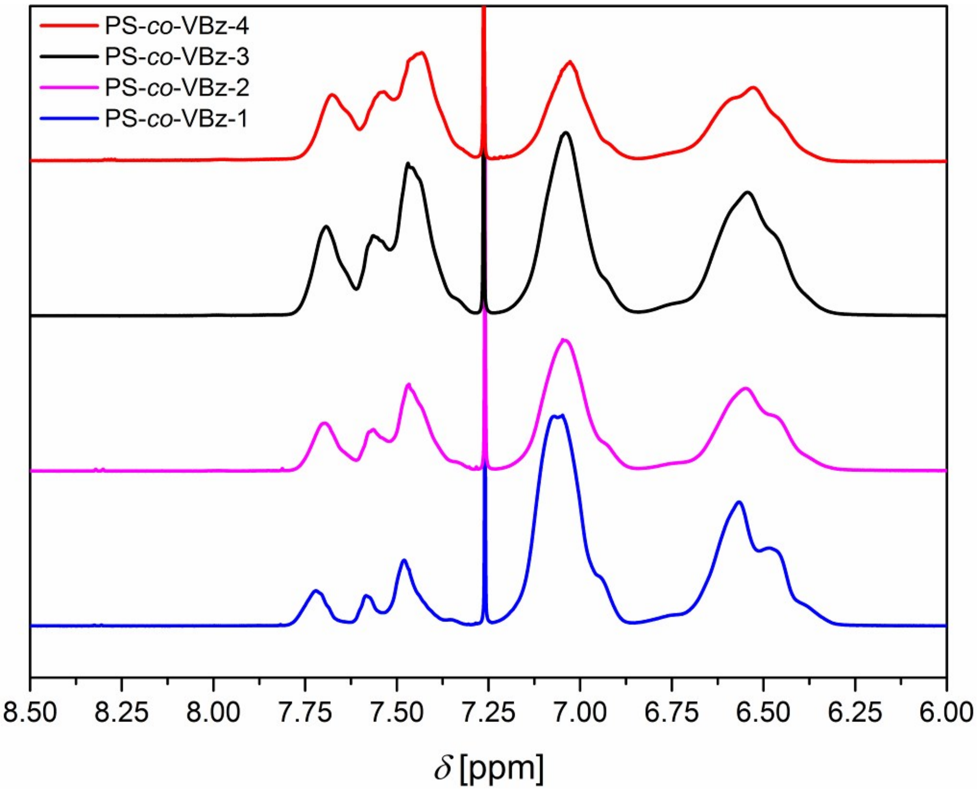

Figure S14. Collection of aromatic regions of ^{1}H-NMR spectra of PS-*co*-VBz in CDCl$_3$ at 500 MHz.

2.5. *RAFT copolymerization of styrene and* SF_5 *(PS*-co-*SF_5)*

Styrene (2.20 g, 21.2 mmol, 977.0 eq.), SF_5 (0.82 g, 4.2 mmol, 193.5 eq.) and BDT (8.0 mg, 0.022 mmol) were dissolved in trifluorotoluene (3.30 g) in a vial. The vial was sealed and the solution was degassed via purging with argon for 15 min. Subsequently, the solution was heated in an oil bath at 110 °C for 19 h. Afterwards the reaction was quenched with liquid nitrogen and the polymers were precipitated twice in an excess of cold methanol. Finally the product was dried in the vacuum oven at 40 °C over night to afford the polymer as a yellow powder (1.20 g). SEC($CHCl_3$): M_n(SEC) = 42300 g mol^{-1}, $Đ$ = 1.35.

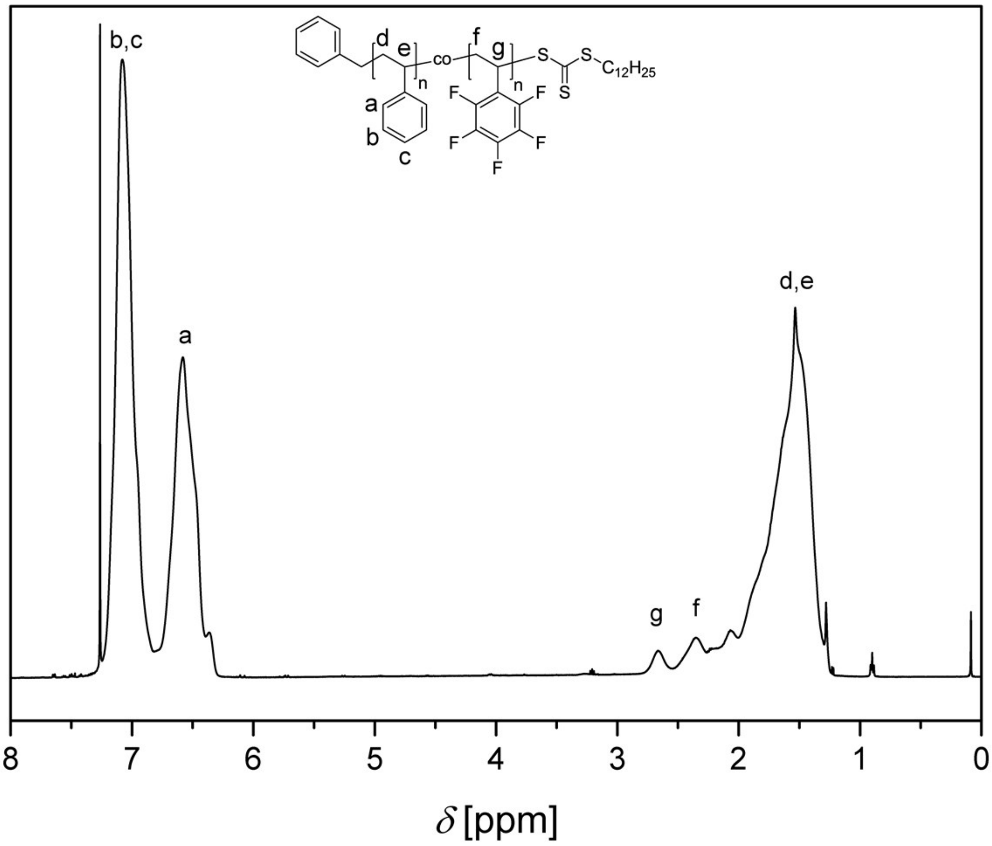

Figure S15. ^{1}H-NMR spectrum of PS-*co*-SF_5 in $CDCl_3$ at 500 MHz.

2.6. *Synthesis of 6-mercapto-1-ferrocene-hexanone (FcSH)*[6]

Ferrocene (4.00 g, 21.50 mmol, 1.0 eq.) was dissolved in dry DCM (40 mL). The mixture was cooled to -15 C in an ice/NaCl bath. 6-Bromo-hexanoxyl chloride (3.4 mL, 22.21 mmol, 1.0 eq.) was added dropwise to a suspension of aluminum trichloride (2.86 g, 21.45 mmol, 1.0 eq.) under stirring. The solution was added dropwise to the ferrocene solution and stirred 2 h at ambient temperature. The reaction mixture was quenched via dropwise addition of water (20 mL). The organic layer was washed with deionized water until the extract was neutral, dried over Na_2SO_4, filtered and the solvent evaporated. The residue was purified via column chromatography on silica gel with a gradual change of the eluent hexane/ethyl acetate from 96% to 68%. The product 6-bromo-1-ferrocene-hexanone was obtained as orange oil (6.75 g, 18.59 mmol, 87%). ^{1}H NMR (500 MHz, $CDCl_3$, δ): 4.78 (t, J=1.9 Hz, 2H; Fc **H**), 4.49 (t, J=1.9 Hz, 2H; Fc-**H**), 4.19 (s, 5H; Fc-**H**), 3.44 (t, J=6.8 Hz, 2H; C**H**$_2$-Br), 2.72 (t, J=7.4 Hz, 2H; C**H**$_2$-C=O), 1.98-1.87 (m, 2H; C**H**$_2$-CH$_2$-C=O), 1.78-1.69 (m, 2H; C**H**$_2$-CH$_2$-Br), 1.61-1.48 (m, 2H; C**H**$_2$).

6-Bromo-1-ferrocene-hexanone (1.08 g, 2.97 mmol, 1.0 eq.) and hexamethyldisilathiane (0.75 mL, 3.59 mmol, 1.2 eq.) were dissolved in dry THF (6 mL) and cooled to -15 °C. A solution of TBAF in THF (1M, 3.3 mL, 3.30 mmol, 1.1 eq.) was added. The mixture was allowed to warm to room temperature over 1.5 h. The reaction was quenched by adding the solution to ice cold water (15 mL). The organic layer was then diluted with Et_2O and washed with water (5x30 mL). The organic layer was collected and dried with $MgSO_4$ and the solvent was removed in vacuo. The crude product was purified via column chromatography on silica gel with a gradual change of the eluent hexane/ethyl acetate from 95% to 60% to afford 6-mercapto-1-ferrocene-hexanone (FcSH) as an orange solid (0.72 g, 2.29 mmol, 77%). ^{1}H NMR (500 MHz, $CDCl_3$, δ): 4.77 (s, 2H; Fc-**H**), 4.49 (s, 2H; Fc-**H**), 4.19 (s, 5H; Fc-**H**), 2.71 (t, J=7.3 Hz, 2H; C**H**$_2$-C=O), 2.56 (m, 2H; C**H**$_2$-SH), 1.81-1.60 (m, 4H; C**H**$_2$-CH$_2$-C=O, C**H**$_2$-CH$_2$-SH), 1.55-1.44 (m, 2H; C**H**$_2$), 1.36 (t, J=7.8 Hz, 1H; S**H**); ^{13}C NMR (126 MHz, CDCl$_3$, δ): 204.2, 79.1, 72.1, 69.7, 69.3, 39.5, 38.8, 33.9, 29.1, 28.4, 28.2, 24.5, 24.1, 23.9. MS (FD) *m*/*z*: $[M]^+$ calcd for $C_{16}H_{20}OSFe$, 316.06; found, 316.05.

*2.7. Pentafluorostyrene-thiol substitution reaction with FcSH (PS-*co*-Fc)*

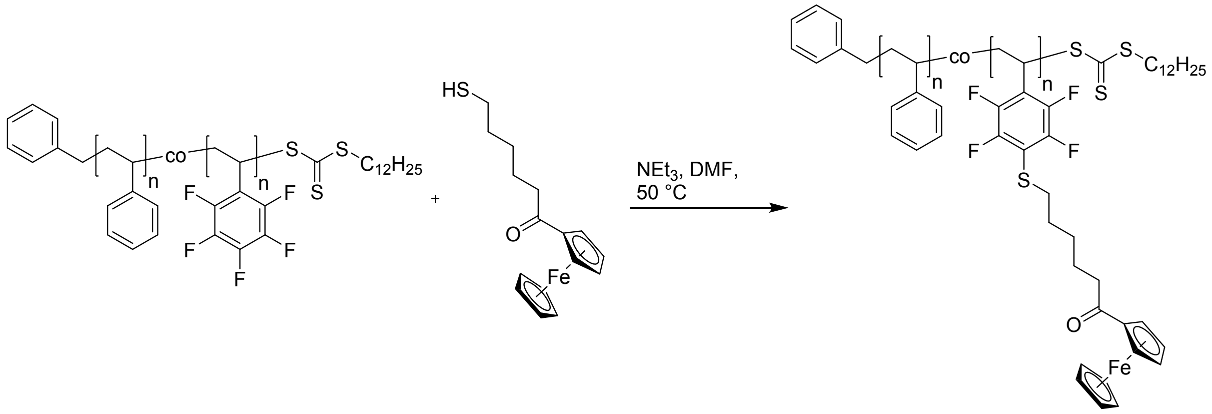

Scheme S3. Synthesis of functionalized polymers: synthesis of ferrocene functionalized PS (PS-*co*-Fc) via thiol-pentafluorophenyl substitution reaction.

Under argon PS-*co*-SF$_5$ (100 mg, 0.0024 mmol, 1.0 eq.) and FcSH (147 mg, 0.46 mmol, 193.0 eq.) were dissolved in DMF (1 mL) that was purged with argon for 20 min prior to use. NEt$_3$ (10 μL) was added and the mixture heated to 50 °C for 24 h. The product was precipitated in an excess of cold methanol, dissolved in a minimum amount of DCM and reprecipitated in an excess of cold methanol. Finally the product was dried in the vacuum oven at 40 °C overnight to yield the product as orange powder (67 mg). A ferrocene incorporation of 15 mol% was calculated according to ^{1}H-NMR. SEC(CHCl$_3$): M_n(SEC) = 50700 g mol^{-1}, $Đ = 1.35$.

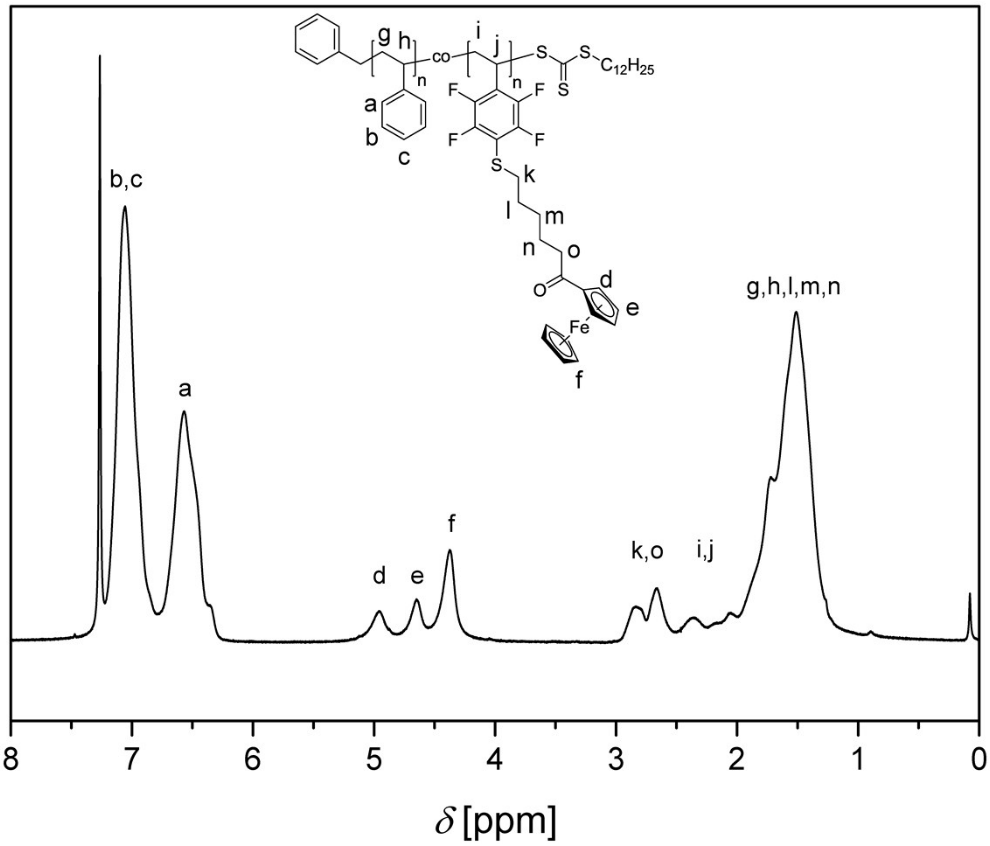

Figure S16. ^{1}H-NMR spectrum of PS-*co*-Fc in $CDCl_3$ at 500 MHz.

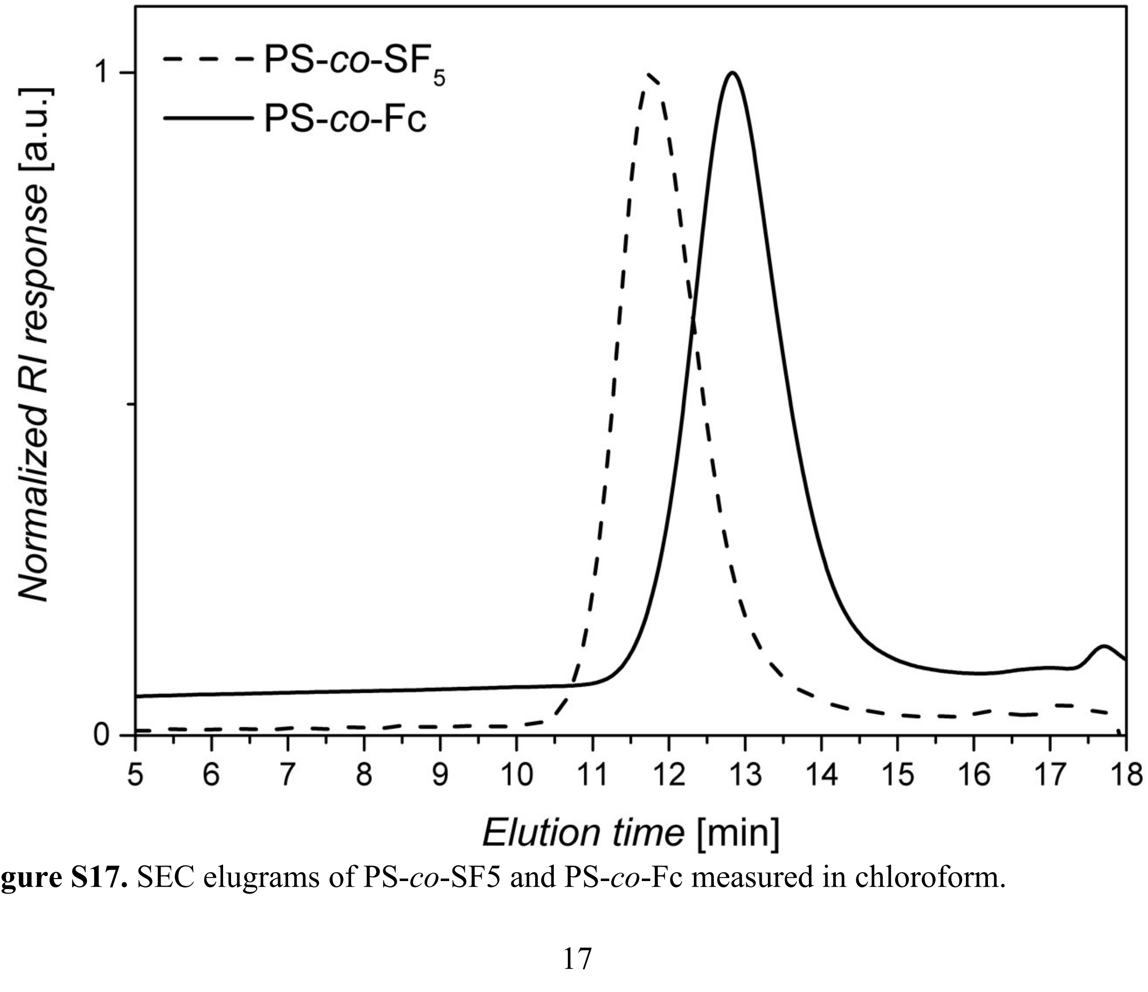

Figure S17. SEC elugrams of PS-*co*-SF5 and PS-*co*-Fc measured in chloroform.

3. Particle synthesis: incorporation of homopolymers

3.1. Particle synthesis using constant surfactant ratio

Table S3. Particle synthesis parameters for particles from blends of PS-*b*-P2VP + *h*-PS and *h*-P2VP with a fixed surfactant ratio (TEM images presented in Figure S3).

PS-*b*-P2VP type	PS-*b*-P2VP fraction [wt.%]	PS type	PS fractions [wt.%]	P2VP type	P2VP fractions [wt.%]	surfactant fractions [wt.%]	
						CTAB	CTEAB-OH
PS_{102}-*b*-$P2VP_{97}$	100	-	0	-	0	30	70
PS_{102}-*b*-$P2VP_{97}$	90	PS_{44}	5	$P2VP_{46}$	5	30	70
PS_{102}-*b*-$P2VP_{97}$	70	PS_{44}	15	$P2VP_{46}$	15	30	70
PS_{102}-*b*-$P2VP_{97}$	50	PS_{44}	25	$P2VP_{46}$	25	30	70
PS_{102}-*b*-$P2VP_{97}$	30	PS_{44}	35	$P2VP_{46}$	35	30	70
PS_{102}-*b*-$P2VP_{97}$	10	PS_{44}	45	$P2VP_{46}$	45	30	70
-	0	PS_{44}	50	$P2VP_{46}$	50	30	70

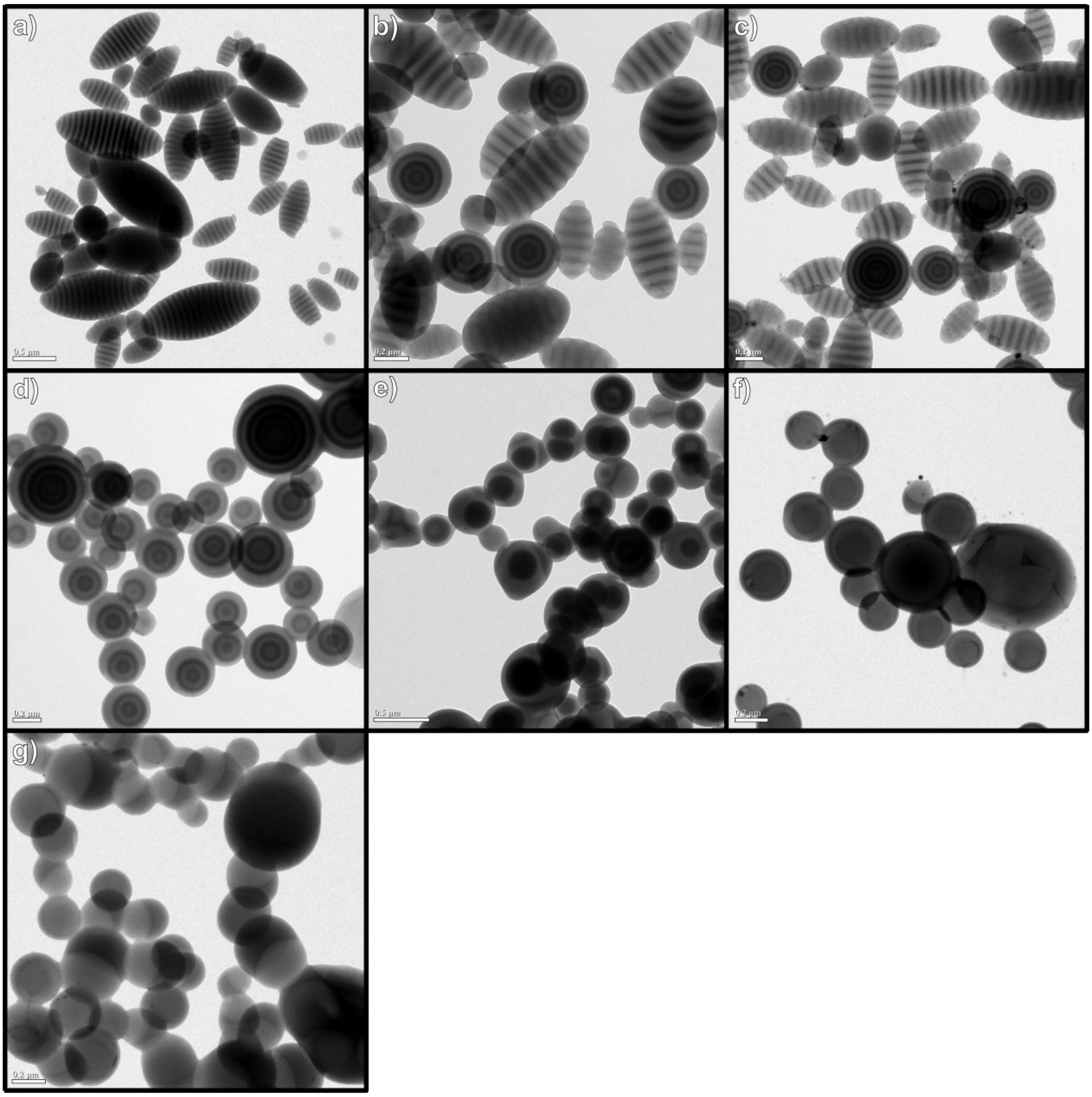

Figure S18: Ellipsoidal particles from blends of PS$_{102}$-*b*-P2VP$_{97,}$ PS$_{44}$ and P2VP$_{46}$ with fixed non-optimized surfactant ratio of CTAB/CTEAB-OH 30/70 wt.%: a) pure block copolymer (scale bar 0.5 µm), b) blend composition 90/5/5 wt.% (scale bar 0.2 µm), c) blend composition 80/15/15 wt.% (scale bar 0.2 µm), d) blend composition 50/25/25 wt.% (scale bar 0.2 µm), e) blend composition 30/35/35 wt.% (scale bar 0.5 µm), f) blend composition 10/45/45 wt.% (scale bar 0.2 µm) and g) blend composition 0/50/50 wt.% (scale bar 0.2 µm).

3.2. Particle synthesis with optimized surfactant ratio

Table S4. Optimized particle synthesis parameters (for particle formations presented in Figure 1-6, Figure S19).

PS$_{102}$-*b*-P2VP$_{97}$ fraction [wt.%]	PS type	PS fractions [wt.%]	P2VP type	P2VP fractions [wt.%]	surfactant fractions [wt.%]	
					CTAB	CTEAB-OH
100	-	0	-	0	31	69
90	PS$_{44}$	5	P2VP$_{46}$	5	25	75
80	PS$_{44}$	10	P2VP$_{46}$	10	30	70
70	PS$_{44}$	15	P2VP$_{46}$	15	32	68

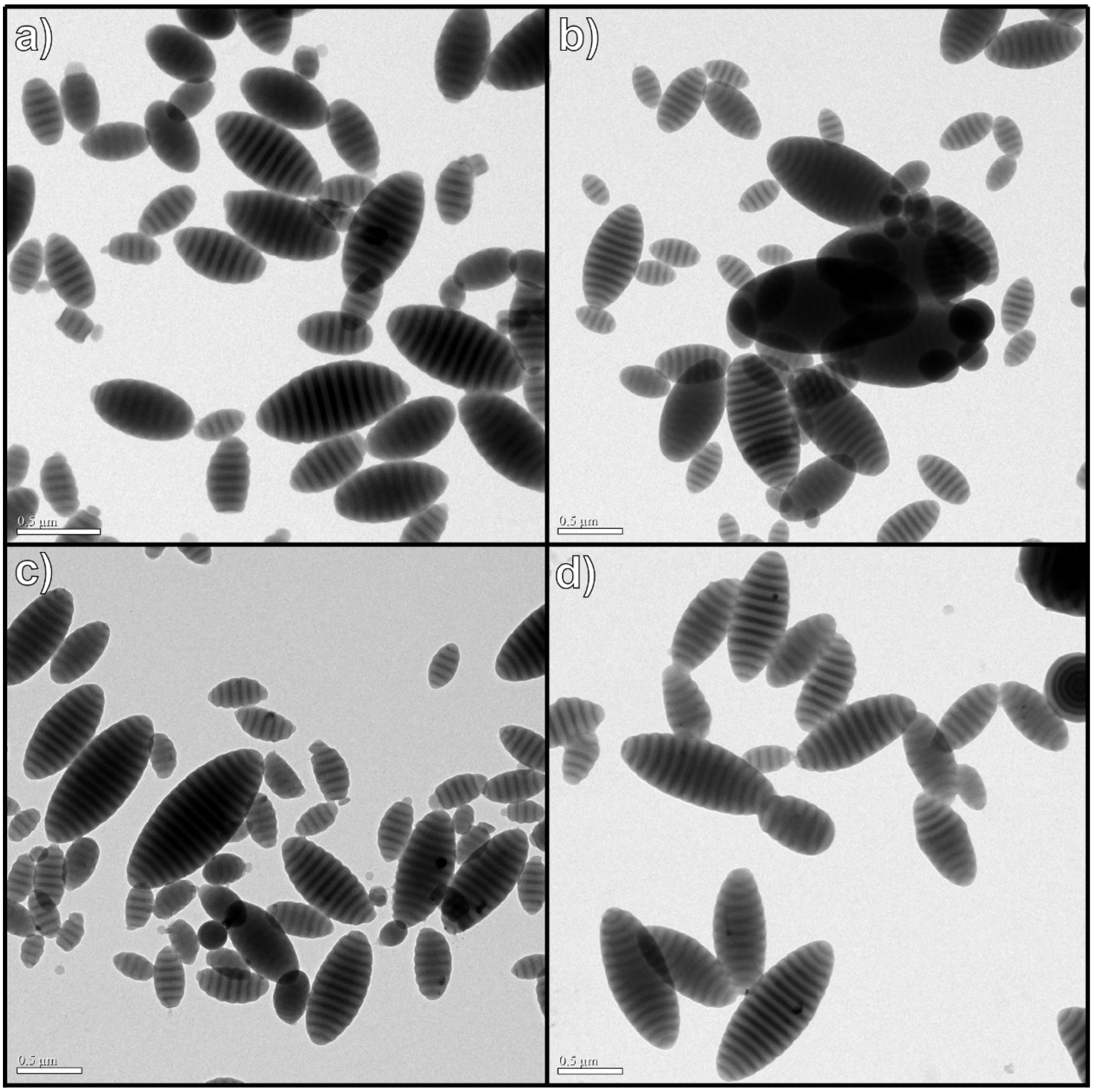

Figure S19. TEM images of ellipsoidal particles from blends of PS$_{102}$-*b*-P2VP$_{97}$, PS$_{44}$ and P2VP$_{46}$ (scale bars 0.5 µm) with optimized surfactant ratios: a) pure block copolymer, b) blend composition 90/5/5 wt.%, c) blend composition 80/10/10 wt.% and d) blend composition 70/15/15 wt.%.

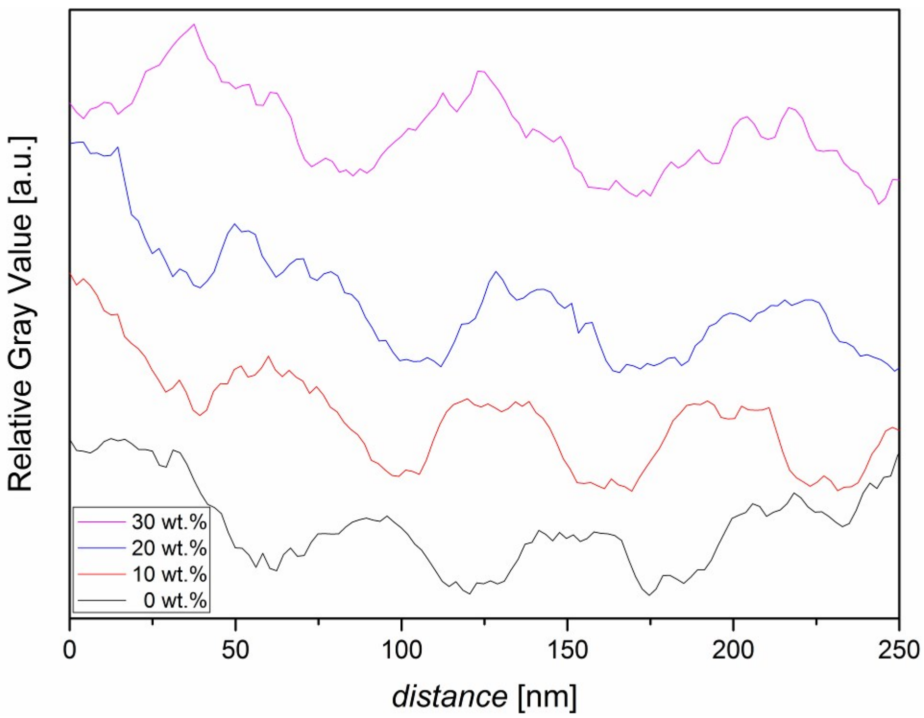

Figure S20. Grayscale profiles from ellipsoid nano particles derived from PS_{102}-*b*-$P2VP_{97}$, PS_{44} and $P2VP_{46}$ with various incorporation ratios.

4. Particle synthesis: incorporation of functional copolymers

4.1. Incorporation of benzophenone copolymers

Table S5. Particle synthesis parameters for particles from blends of PS-*b*-P2VP + PS-*co*-VBz and P2VP-*co*-VBz (TEM images presented in Figure S21, Figure S22, Figure S23).

PS-*b*-P2VP type	PS-*b*-P2VP fraction [wt.%]	PS type	PS fractions [wt.%]	P2VP type	P2VP fractions [wt.%]	surfactant fractions [wt.%]	
						CTAB	CTEAB-OH
PS$_{102}$-*b*-P2VP$_{97}$	90	PS-*co*-VBz-1	5	P2VP-*co*-VBz-1	5	28	72
PS$_{102}$-*b*-P2VP$_{97}$	80	PS-*co*-VBz-1	10	P2VP-*co*-VBz-1	10	28	72
PS$_{102}$-*b*-P2VP$_{97}$	70	PS-*co*-VBz-1	15	P2VP-*co*-VBz-1	15	28	72
PS$_{102}$-*b*-P2VP$_{97}$	90	PS-*co*-VBz-2	5	P2VP-*co*-VBz-2	5	28	72
PS$_{102}$-*b*-P2VP$_{97}$	80	PS-*co*-VBz-2	10	P2VP-*co*-VBz-2	10	28	72
PS$_{102}$-*b*-P2VP$_{97}$	70	PS-*co*-VBz-2	15	P2VP-*co*-VBz-2	15	28	72
PS$_{102}$-*b*-P2VP$_{97}$	90	PS-*co*-VBz-3	5	P2VP-*co*-VBz-3	5	28	72
PS$_{102}$-*b*-P2VP$_{97}$	80	PS-*co*-VBz-3	10	P2VP-*co*-VBz-3	10	28	72
PS$_{102}$-*b*-P2VP$_{97}$	70	PS-*co*-VBz-3	15	P2VP-*co*-VBz-3	15	28	72
PS$_{102}$-*b*-P2VP$_{97}$	90	PS-*co*-VBz-4	5	P2VP-*co*-VBz-4	5	28	72
PS$_{102}$-*b*-P2VP$_{97}$	80	PS-*co*-VBz-4	10	P2VP-*co*-VBz-4	10	28	72
PS$_{102}$-*b*-P2VP$_{97}$	70	PS-*co*-VBz-4	15	P2VP-*co*-VBz-4	15	28	72
PS$_{102}$-*b*-P2VP$_{97}$	80	PS$_{44}$	10	P2VP-*co*-VBz-1	10	30	70
PS$_{102}$-*b*-P2VP$_{97}$	80	PS$_{44}$	10	P2VP-*co*-VBz-2	10	28	72
PS$_{102}$-*b*-P2VP$_{97}$	80	PS$_{44}$	10	P2VP-*co*-VBz-4	10	30	70
PS$_{102}$-*b*-P2VP$_{97}$	80	PS-*co*-VBz-1	10	P2VP$_{46}$	10	30	70
PS$_{102}$-*b*-P2VP$_{97}$	80	PS-*co*-VBz-2	10	P2VP$_{46}$	10	28	72
PS$_{102}$-*b*-P2VP$_{97}$	80	PS-*co*-VBz-4	10	P2VP$_{46}$	10	28	72

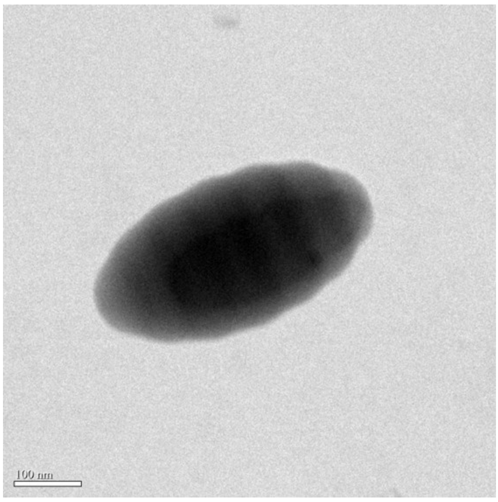

Figure S21. TEM image of a control sample of ellipsoid nano particles without staining.

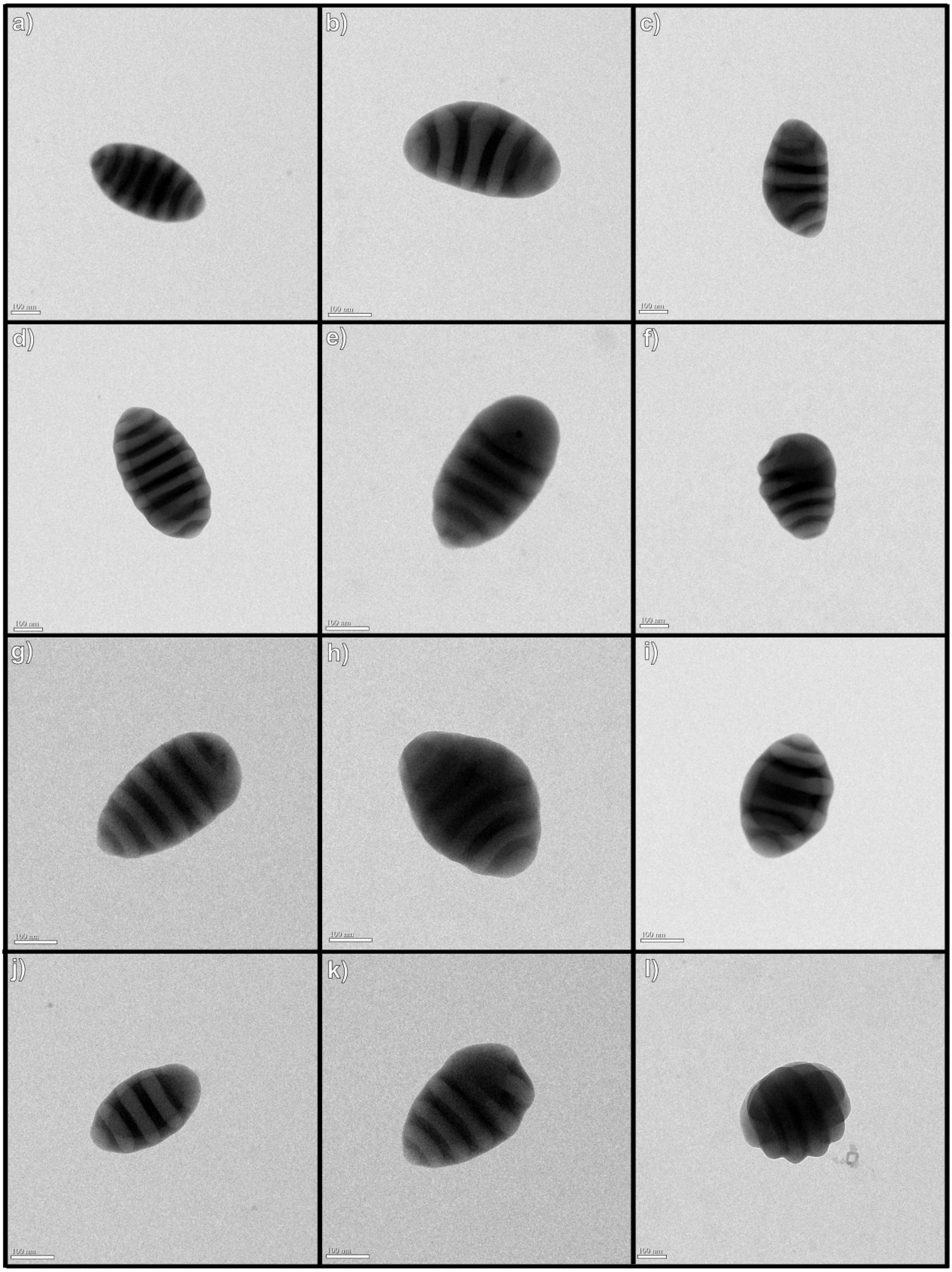

Figure S22. TEM images of crosslinked nano particles (scale bars 0.1 µm) formed with optimized surfactant ratio of CTAB/CTEAB-OH 28/72 wt.%: PS_{102}-*b*-$P2VP_{97}$, PS-*co*-VBz-1 and P2VP-*co*-VBz-1 (blend ratios a) 90/5/5 wt.%, b) 80/10/10 wt.% and c) 70/15/15 wt.%); PS_{102}-*b*-$P2VP_{97}$, PS-*co*-VBz-2 and P2VP-*co*-VBz-2 (blend ratios d) 90/5/5 wt.%, e) 80/10/10 wt.% and f) 70/15/15 wt.%); PS_{102}-*b*-$P2VP_{97}$, PS-*co*-VBz-3 and P2VP-*co*-VBz-3 (blend ratios g) 90/5/5 wt.%, h) 80/10/10 wt.% and i) 70/15/15 wt.%); PS_{102}-*b*-$P2VP_{97}$, PS-*co*-VBz-4 and P2VP-*co*-VBz-4 (blend ratios j) 90/5/5 wt.%, k) 80/10/10 wt.% and l) 70/15/15 wt.%).

4.2. *Investigations on swelling properties of crosslinked particles*

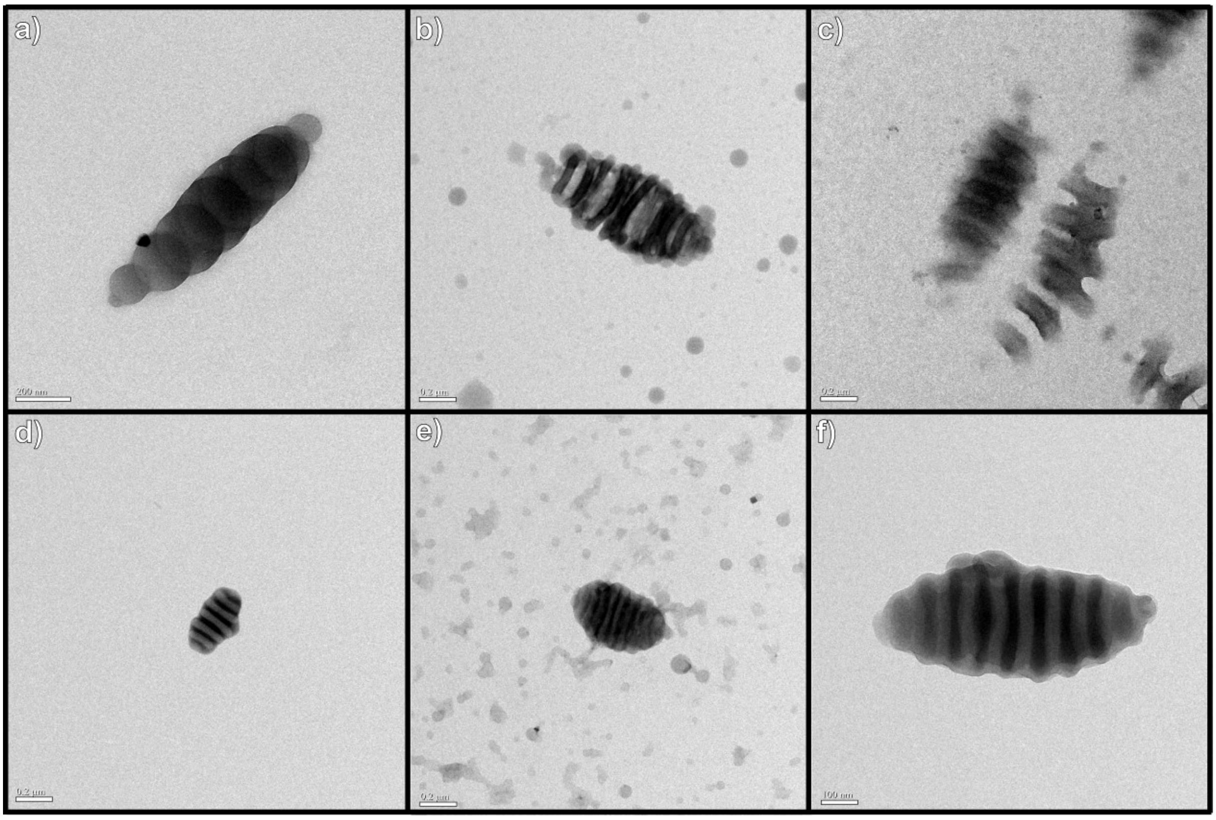

Figure S23. TEM images of nano particles from PS_{102}-*b*-$P2VP_{97}$ (90 wt.%), PS-*co*-VBz-1 (5 wt.%) and P2VP-*co*-VBz-1 (5 wt.%) (scale bars 0.2 µm except f) with 0.1 µm): after adjusting the pH to 3 and after neutralization (a and d), after swelling in acetone and deswelling (b and e) and after swelling in cyclohexane and deswelling (c and f).

4.3. *Particles with crosslinked P2VP domains and ferrocene-functionalized PS domains*

Table S6. Particle synthesis parameters for particles from blends of PS-*b*-P2VP + PS-*co*-Fc and P2VP-*co*-VBz.

PS_{102}-*b*-$P2VP_{97}$ fraction [wt.%]	PS type	PS fractions [wt.%]	P2VP type	P2VP fractions [wt.%]	surfactant fractions [wt.%]	
					CTAB	CTEAB-OH
90	PS-*co*-Fc	5	P2VP-*co*-VBz-1	5	22	78

4.4. Infiltration of Au nanoparticles into P2VP domains

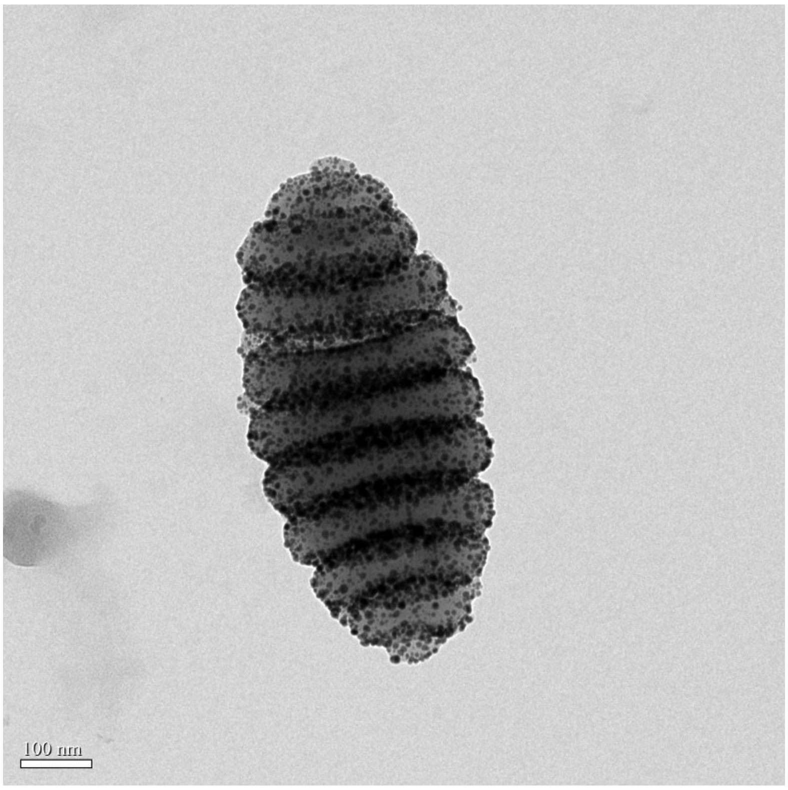

Figure S24. Au nano particle incorporation into crosslinked ellipsoid nanoparticles via swelling of the P2VP phases, introduction of Au^{3+} ions, deswelling and reduction via $NaBH_4$.

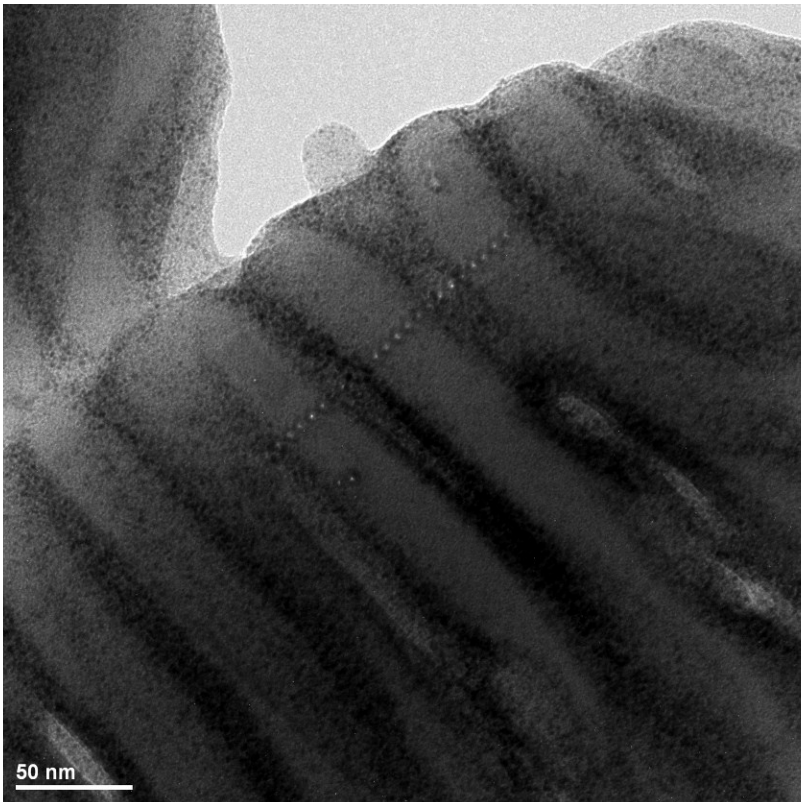

Figure S25. TEM image of ellipsoid nano particles with ferrocene and Au nano particle incorporation after EDX measurement perpendicular to the polymer domains.

4.5. Introduction of ferrocene into reactive PS domains

Table S7. Particle synthesis parameters for particles from blends of PS-*b*-P2VP + PS-*co*-PSF$_5$ + PS-*co*-VBz and P2VP-*co*-VBz.

PS$_{102}$-*b*-P2VP$_{97}$ fraction [wt.%]	PS type	PS fractions [wt.%]	P2VP type	P2VP fractions [wt.%]	surfactant fractions [wt.%]	
					CTAB	CTEAB-OH
80	PS-*co*-PSF$_5$; PS-*co*-VBz-1	5/5	P2VP-*co*-VBz-1	10	28	72

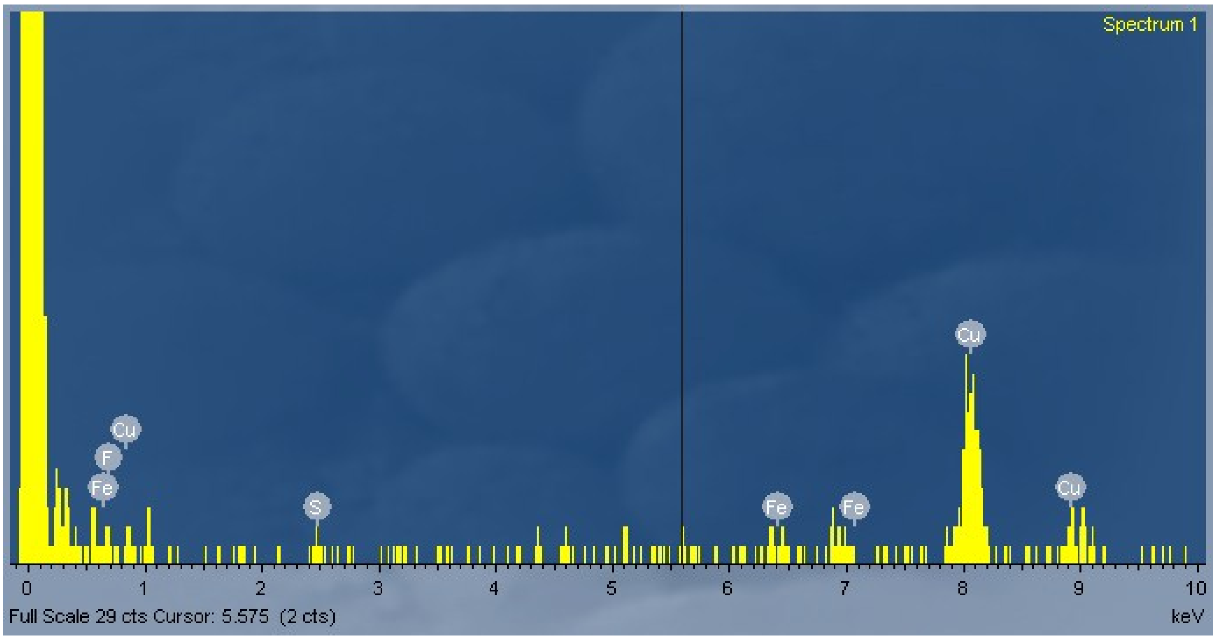

Figure S26. EDX spectrum of nanoparticles obtained from PS-*co*-SF$_5$, PS-*co*-VBz-1, P2VP-*co*-VBz-1 and PS$_{102}$-*b*-P2VP$_{97}$ after crosslinking, swelling, functionalization with Fc-SH and deswelling.

5. References

1. Klinger, D.; Wang, C. X.; Connal, L. A.; Audus, D. J.; Jang, S. G.; Kraemer, S.; Killops, K. L.; Fredrickson, G. H.; Kramer, E. J.; Hawker, C. J., *Angew. Chem., Int. Ed.* **2014,** *53* (27), 7018-7022. DOI 10.1002/anie.201400183.
2. Schmidt, B. V. K. J.; Hetzer, M.; Ritter, H.; Barner-Kowollik, C., *Macromolecules* **2011,** *44* (18), 7220-7232. DOI 10.1021/ma2011969.
3. Skey, J.; O'Reilly, R. K., *Chem. Commun.* **2008,** (35), 4183-4185. DOI Doi 10.1039/B804260h.
4. Denmark, S. E.; Butler, C. R., *Org. Syn,* **2009,** *86*, 274.
5. Chen, Y.; Tavakley, A. E.; Mathiason, T. M.; Taton, T. A., *J. Polym. Sci., Part A: Polym. Chem.* **2006,** *44* (8), 2604-2614. DOI 10.1002/pola.21367.
6. Tindale, J. J.; Hartlen, K. D.; Alizadeh, A.; Workentin, M. S.; Ragogna, P. J., *Chem. – Eur. J.* **2010,** *16* (30), 9068-9075. DOI 10.1002/chem.200902610.